

# DFT and EPR study of spin-assisted processes in poly(3-alkylthiophene) oligomers and their composites

V.I. Krinichnyi

Department of Kinetics and Catalysis, Federal Research Center of Problems of Chemical Physics and Medicinal Chemistry RAS, Academician Semenov Avenue 1, Chernogolovka, Moscow Region 142432, Russian Federation

## ARTICLE INFO

### Keywords:

Aromatic additive  
DFT  
EPR  
Oligomer  
Poly(3-Alkylthiophene)  
Self-assembly crystallization

## ABSTRACT

Correlations of spin, electronic and magnetic resonance parameters of charge carriers stabilized in poly(3-alkylthiophene) oligomers with their band structure, polymerization degree, side substitutes, and conformation established by using the density functional theory and electron paramagnetic resonance methods. The comparison of calculated and experimental data identified spin distribution on oligomer chains with different conformations. The type and size of alkyl substituent of polymer matrix governs the band gap, mobility, and spin-orbit coupling of polaron charge carriers. The introduction of small aromatic additives between oligomer chains initiates their self-assembly crystallization and formation of organic:organic spinterface which accelerates spin-assisted electronic and magnetic processes in the composite. The research revealed that embedding aromatic hydrocarbons into oligomer bulk allows continuous and discrete handling of electronic spin-assisted processes carrying out in respective organic/organic composites. The key role of spinterface effects in the development of a new generation of molecular devices with actively tuned spin-assisted functionality is described.

## 1. Introduction

Organic conjugated polymers with an extended  $\pi$ -structure are synthesized and studied in many labs due to the prospects of their use as active matrices in new generation of electronic, photonic and spintronic devices with spin-dependent properties, for example, solar energy converters and batteries, nonlinear optics elements, band filters, fluorescent probes and sensors [1–3]. Polythiophene derivatives, regioregular poly(3-alkylthiophenes) (P3AT) with various side alkyl substituents, polypyrrole, polyaniline, other conjugated polymers are widely used as a matrix of respective donor-accepter composites. They are considered also as optimal model systems for establishing fundamental spin-dependent processes of charge initiation, separation and recombination in different organic polymer systems. It was shown [4–6] that interfacial synthesis of conjugated polymers in the presence of carbon nanotubes, graphene, other aromatic additives allows obtaining nanocomposites with improved optical and electronic parameters.

The energy in organic polymer systems is carried by topological distortions, quasiparticles, paramagnetic polarons and/or diamagnetic bipolarons with single and double elemental charge, respectively [7]. The width of polarons and bipolarons in conjugated polymers is usually 3–5 and 5–6 polymer units, respectively [8–10]. Polaron pairs are well

separated by radical ions not only in P3AT but also in respective oligomers. The stability of polarons over bipolarons formed in oligothiophene was determined [11] to be inversely proportional to chain length. A partial localization of bipolarons identified on this oligomer seems to be similar to the pinning of charge carriers in other quasi-one-dimensional (Q1D) conjugated systems [12]. Such charge carriers play an important role not only in organic conjugated polymers, but also in some inorganic semiconductors, e.g., GaAs [13] and ABO<sub>3</sub> perovskites [14]. Most of the processes occurring in these systems depend on the number, dynamics, and relaxation of such quasiparticles. Indeed, their comprehensive study has revealed correlations of their electronic parameters on structure, composition, morphology, as well as an external influence.

Spin nature of carriers transferring a charge opens conceptually new class of devices in which molecular hybrid interfaces play an active role improving their controllability as well as physical and chemical functionalities [15]. The carriers are transferred through donor-accepter interface with the probability determined by the spin-polarization of the density of states at the Fermi level  $E_F$ . Because their spins may be orientated along and opposite to the direction of external magnetic field, new spin-filter with hybrid electronic states forms at such element. In order such spinterfaces could supply principally new detailed

E-mail addresses: [kivirus@gmail.com](mailto:kivirus@gmail.com), [kivi@icp.ac.ru](mailto:kivi@icp.ac.ru).

<https://doi.org/10.1016/j.synthmet.2024.117596>

Received 17 November 2023; Received in revised form 20 March 2024; Accepted 24 March 2024

Available online 30 March 2024

0379-6779/© 2024 Elsevier B.V. All rights reserved.

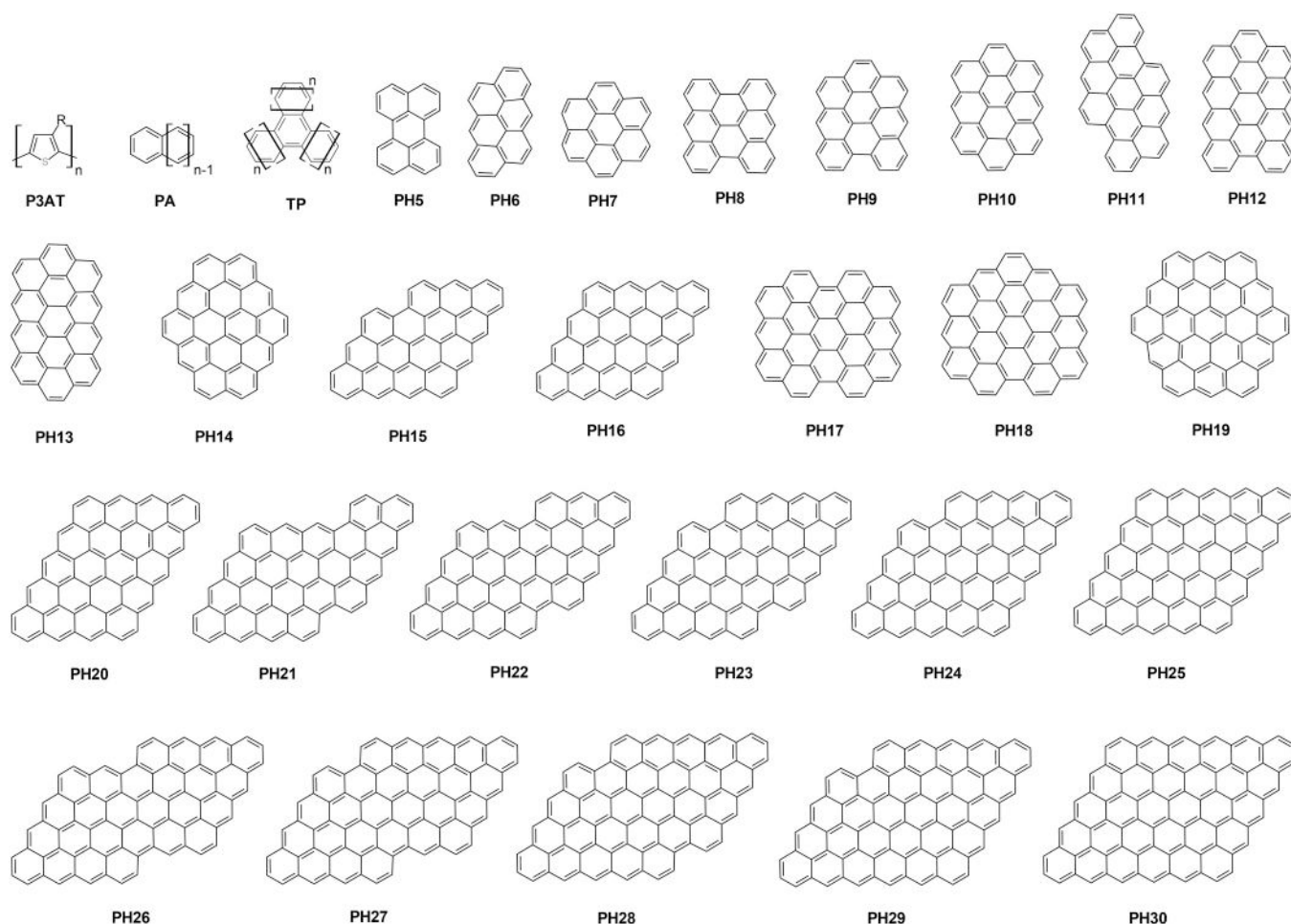


**Fig. 1.** Poly(3-Alkylthiophene) (P3AT,  $A=R=C_mH_{2m+1}$ ) oligo- $n$ -mers, poly(3-hydrothiophene) (P3HyT,  $R=H$ ,  $m=0$ ), poly(3-methylthiophene) (P3MeT,  $R=Me$ ,  $m=1$ ), poly(3-ethylthiophene) (P3EtT,  $R=Et$ ,  $m=2$ ), poly(3-buthylthiophene) (P3BuT,  $R=Bu$ ,  $m=4$ ), poly(3-hexylthiophene) (P3HxT,  $R=Hx$ ,  $m=6$ ), poly(3-octylthiophene) (P3OcT,  $R=Oc$ ,  $m=8$ ), poly(3-decylthiophene) (P3DeT,  $R=De$ ,  $m=10$ ), and poly(3-dodecylthiophene) (P3DoT,  $R=Do$ ,  $m=12$ ), as well as quasi-one-dimensional (Q1D) polyacenes (PA), triphenylenes (TP), and quasi-two-dimensional (Q2D) graphene-like polycyclic aromatic hydrocarbons (PH) with different number of benzene circles and extended  $\pi$ - $\pi^*$ -structures used in the work. For simplicity, hydrogen atoms are not shown.

information about electronic processes, they should be converted into an extraordinary element able to continual control the hybridized layer during selective and tunable excitations by, e.g., illumination and/or electric or magnetic field. The spin-assisted electronic configuration has been mainly investigated in some model organic/inorganic interfaces [16–18]. Despite the high promise of using fully organic donor-acceptor systems for this purpose, today, however, is known little about respective investigations and applications.

Various methods can be used for the study of conjugated polymers and their composites. Detailed information about excited states, excitons, can be obtained, e.g., by polarization optical dichroism, while various anisotropic interactions occurring in these compounds can be successfully analyzed using high-resolution nuclear magnetic resonance (NMR) spectroscopy. The spin nature of charge carriers expectedly predetermined the wide use for such purpose the direct electron paramagnetic resonance (EPR) spectroscopy. Magnetic resonant methods allow to determine the main parameters of the spin Hamiltonian of polaron radical ions and triplet states formed upon doping or photoexcitation of polymer systems [19–25]. Besides, EPR method allows one to obtain more accurate information about the features of electron-electron, electron-nuclear and electron-phonon interactions, relaxation properties, as well as the distribution of spin and electron density spread along charge carriers. Despite numerous studies, to date, however, it has not been possible to obtain unambiguous information about the nature of excited states, as well as the mechanisms of spin-spin

interactions and electronic relaxation. This is mainly limited by the variety of polymer synthesis, its stability, as well as the peculiarities of experimental methods. The interpretation of experimental results is also limited due to monomeric rotation in aromatic polymers near own main  $x$ -axis. This increases a torsion/dihedral angle between monomer planes, e.g., up to near  $150^\circ$  in polythiophene or poly(3-hydrothiophene) (P3HyT) [26]. This makes it difficult to transfer charge along this axis and accelerates its recombination process. When analyzing the results obtained, it is also necessary to take into account possible formation of energetically deep spin traps spatially distributed in a real polymer matrix. This requires the study of conjugated oligomers using a combination of various experimental and theoretical approaches. Previously, the possibility of spatial orientation of an elongated conjugated oligomer by embedding it into a liquid crystal matrix was demonstrated [27]. This study of oriented thin films of oligothiophenes with different chain lengths show that the main  $\pi$ - $\pi^*$ -transition is directed parallel to the main molecular  $x$ -axis. This opens up the way of subsequent detailed study of the structural and electronic properties of oligomers, polymers, and corresponding composites. By changing the spin state of a donor-acceptor system, for example, under illumination, it becomes possible to handle the width of its band gap and, thus, control the thermal transfer of the initiated charge from the valence band to the conduction band of the molecular compound [28].

Numerical calculations of the structural and energetic properties of various oligomers can be realized within the framework of the electron

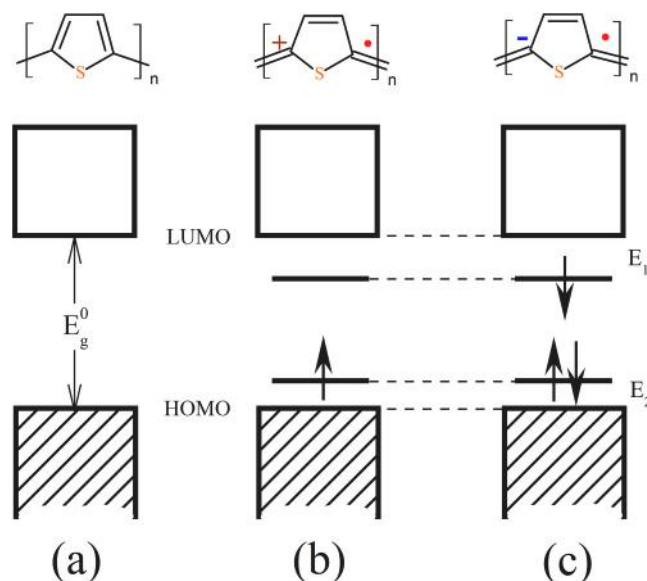


**Fig. 2.** Evolution of the band structure of neutral poly(3-hydrothiophene) with band gap  $E_g^0$  (a) upon leaving its backbone of elemental charge  $|e|$ , accompanied by the formation of polarons  $P^{+*}$  (b) or  $P^{-*}$  (c) with respective energy sublevels  $E_i$  in the band gap.

density functional theory (DFT) formalism [29]. Thus, the band gap energy,  $E_g$ , of neutral P3HyT was determined within such approach as the difference between the energies of its highest occupied molecular orbital (HOMO) and lowest unoccupied molecular orbital (LUMO),  $E_g = E_{LUMO} - E_{HOMO}$ , which appeared to be equal to 2.20 eV [30]. A significant decrease in this parameter was obtained upon the transformation of its aromatic isomers into quinoid form [31]. In the present work was used the Orca package [32] with a wide range of different quantum chemical approaches, including the DFT formalism. In contrast with the well-known GAUSSIAN and other quantum calculation programs, free distributing simple Orca package with a wide range of different approaches was appeared to be most flexible, quite effective in calculation speed and RAM used for complex and resource-intensive quantum chemical calculations. This becomes especially important in the study of atomic and molecular systems with open shells including polymer donor-accepter composites with spin charge carriers. Its usage, for instance, with the EPRNMR module allows one fast and directly compute and control the Landé splitting, hyperfine coupling, other magnetic resonance parameters of open-shell solids in parallel multi-process mode. Indeed, corresponding calculations of paramagnetic compounds using this program in other centers allowed to obtain more adequate and informative parameters of paramagnetic centers in different polymer systems, see, e.g., [24,33].

Previously, numerous DFT and experimental EPR studies of donor-acceptor systems allowed us to establish an increase in their photovoltaic efficiency when introduced into their polymer matrix of small aromatic additives [34,35]. Such interfacial effect was appeared to grow inversely exponentially with a band gap of additives which play a role of template for heteroepitaxial self-assembly crystalline phase of polymer

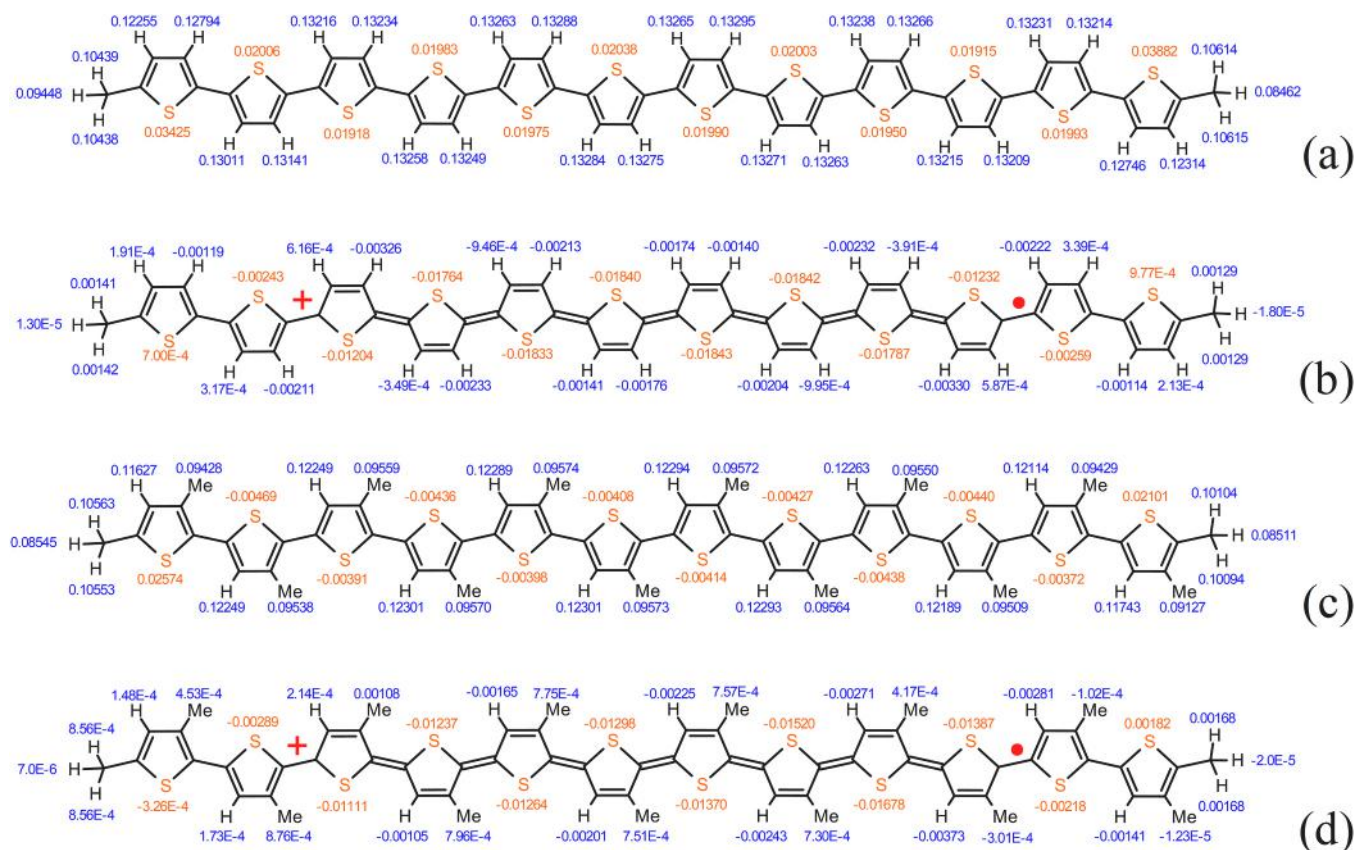


**Fig. 3.** Charge density (a,c) and spin population (b,d) on the hydrogen and methyl substitutes and sulphur nuclear in the DFT optimized neutral and oxidized polythiophene (a,b) and poly(3-methylthiophene) (c,d) 12-oligomers calculated according the Mulliken approach using the Orca software package with B3LYP functional, EPRNMR module for  $^{12}\text{C}$  and  $^1\text{H}$ , TZVPP basis set for  $^{32}\text{S}$ , and EPRNMR module. The polarons with spin  $S=1/2$ , elemental positive charge  $+e$ , and 8-unit quinoid conformation are shown in b and d. The mean respective parameters of all hydrogen nuclei of methyl substituents are shown in c and d. More details of the DFT calculation are described in Methodical section.

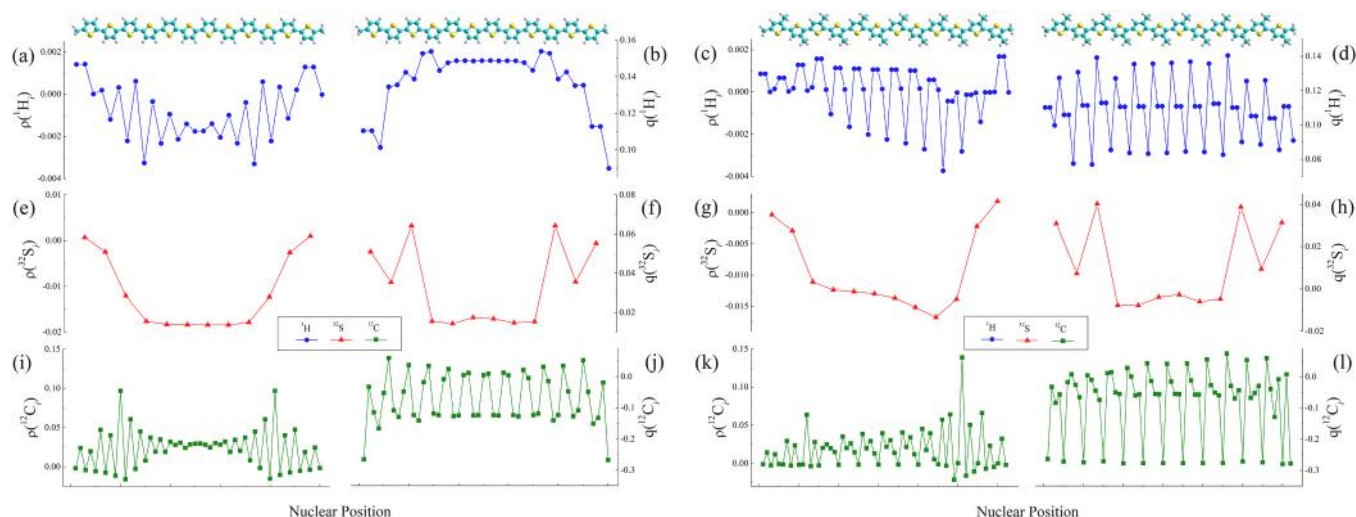


**Fig. 4.** Spin population (a,e,i,c,g,k) and charge density (b,f,j,d,h,l) on the hydrogen  $^1\text{H}$  (circles), sulfur  $^{32}\text{S}$  (triangles), and carbon  $^{12}\text{C}$  (squares) nuclei of the poly(3-hydrothiophene) (left) and poly(3-methylthiophene) (right) oligo12mers (shown schematically in the top) possessing overall spin  $S=1/2$  and an elemental positive charge  $+e$  calculated according the Mulliken approach using the Orca software package with B3LYP functional, 6–311 G basis set for  $^1\text{H}$  to  $^{12}\text{C}$ , TZVPP one for  $^{32}\text{S}$ , and EPRNMR module. The details of the calculations are discussed in the Methodical section.

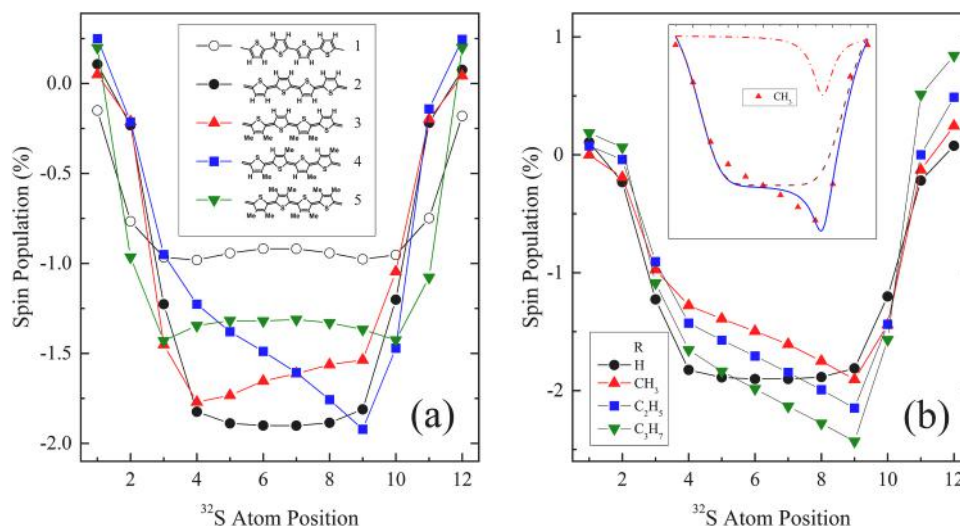


**Fig. 5.** (a) Effective distribution of spin population on the sulfur atoms  $^{32}\text{S}$  along a polaron formed in the P3AT oligo12mers with different combination of side substituents. (b) Spatial distribution of the spin density along polarons formed in some P3AT oligo12mers. The dashed and dash-dotted lines in the insert show the broad- and narrow-band contributions with an integral ratio of 11.2:1.0 into the total spin density on polaron shown by a solid line.

matrix.

In this work, the results of a detailed comparative DFT and EPR study of spin-assisted molecular, structural and magnetic resonance parameters of various P3AT oligomers with polaron charge carriers are discussed. They are compared with those experimentally obtained for various Q1D organic semiconductors and their composites. For isolated chains, good agreement between theoretically calculated and experimentally registered was demonstrated. A potential handling of the spin state and electronic properties of the studied P3AT modified with Q1D polyacenes, as well as quasi-two-dimensional (Q2D) triphenylenes and polycyclic aromatic hydrocarbons is proposed.

## 2. Methodical section

### 2.1. Materials used in the study

In the work the following oligomers of poly(3-alkylthiophenes) (P3AT, where  $A=R=C_m\text{H}_{2m+1}$ , see Fig. 1) were studied: poly(3-

hydrothiophene) (P3HyT,  $m=0$ ), poly(3-methylthiophene) (P3MeT,  $m=1$ ), poly(3-ethylthiophene) (P3EtT,  $m=2$ ), poly(3-butylthiophene) (P3BuT,  $m=4$ ), poly(3-hexylthiophene) (P3HxT,  $m=6$ ), poly(3-octylthiophene) (P3OcT,  $m=8$ ), poly(3-decylthiophene) (P3DeT,  $m=10$ ), and poly(3-dodecylthiophene) (P3DoT,  $m=12$ ) with the monomer number  $n=1-12$ , aromatic and quinoid conformation, in the absence and presence of polarons with spin  $S=1/2$  and positive elementary charge  $+e$ . In order to analyze the effect of polycyclic aromatic hydrocarbons on the electronic and spin properties of 7-dimensional oligomers P3HyT and P3MeT, Q1D polyacenes, benzene ( $n=1$ ), naphthalene ( $n=2$ ), anthracene ( $n=3$ ), tetracene ( $n=4$ ), pentacene ( $n=5$ ), hexacene ( $n=6$ ), heptacene ( $n=7$ ), octacene ( $n=8$ ), nonacene ( $n=9$ ), and decacene ( $n=10$ ) polyacenes (PA) as well as Q2D triphenylenes (TP) with  $n=1-4$  and polyaromatic hydrocarbons (PH) with  $n=5-30$ . These compounds are shown in Fig. 1 without hydrogen atom.

**Table 1**

Band parameters HOMO, LUMO, and  $E_g$  (all in eV) calculated for the initial and oxidized poly(3-alkylthiophene) oligomers with various number of units  $n$  using Orca software package according to the procedure described in the Methodical section.

$n$	HOMO <sup>a</sup>	LUMO <sup>a</sup>	$E_g^a$	HOMO <sup>b</sup>	LUMO <sup>b</sup>	$E_g^b$	HOMO <sup>c</sup>	LUMO <sup>c</sup>	$E_g^c$
Poly(3-Hydrothiophene)									
1	-5.513	-0.501	5.012	-11.923	-6.562	5.362	-12.206	-6.288	5.918
2	-4.951	-1.423	3.528	-9.873	-6.136	3.737	-11.223	-8.172	3.051
3	-4.749	-1.851	2.898	-8.870	-5.828	3.042	-9.732	-7.495	2.237
4	-4.655	-2.094	2.561	-8.246	-5.576	2.670	-8.797	-7.070	1.727
5	-4.608	-2.247	2.361	-7.814	-5.367	2.447	-8.159	-6.778	1.381
6	-4.586	-2.349	2.237	-7.494	-5.192	2.302	-7.692	-6.566	1.126
7	-4.577	-2.420	2.157	-7.246	-5.043	2.204	-7.336	-6.406	0.930
8	-4.576	-2.470	2.106	-7.047	-4.911	2.136	-7.053	-6.281	0.772
9	-4.581	-2.507	2.074	-6.882	-4.792	2.090	-6.824	-6.180	0.644
10	-4.588	-2.534	2.054	-6.741	-4.683	2.059	-6.634	-6.096	0.538
11	-4.597	-2.554	2.043	-6.621	-4.582	2.039	-6.476	-6.025	0.451
12	-4.606	-2.569	2.037	-6.582	-4.561	2.021	-6.381	-5.975	0.406
Poly(3-Methylthiophene)									
1	-5.640	-0.079	5.560	-11.840	-5.969	5.872	-11.853	-9.467	2.386
2	-5.124	-0.960	4.164	-9.880	-5.504	4.376	-10.654	-8.195	2.459
3	-4.923	-1.351	3.572	-8.888	-5.181	3.707	-9.417	-7.545	1.872
4	-4.824	-1.570	3.254	-8.269	-4.926	3.343	-8.531	-7.137	1.394
5	-4.810	-1.722	3.088	-7.867	-4.727	3.139	-7.941	-6.889	1.052
6	-4.855	-1.841	3.014	-7.601	-4.567	3.034	-7.535	-6.745	0.790
7	-4.856	-1.914	2.942	-7.359	-4.415	2.944	-7.213	-6.596	0.616
Poly(3-Ethylthiophene)									
1	-5.590	-0.193	5.397	-11.727	-5.961	5.766	-11.775	-9.336	2.439
2	-5.082	-0.944	4.138	-9.769	-5.415	4.355	-10.550	-8.077	2.472
3	-4.879	-1.344	3.535	-8.782	-5.108	3.673	-9.338	-7.434	1.904
4	-4.781	-1.586	3.195	-8.171	-4.882	3.288	-8.464	-7.032	1.431
5	-4.727	-1.740	2.987	-7.744	-4.696	3.048	-7.860	-6.756	1.104
6	-4.710	-1.821	2.889	-7.434	-4.511	2.923	-7.419	-6.563	0.856
7	-4.689	-1.904	2.785	-7.182	-4.384	2.798	-7.088	-6.399	0.689
Poly(3-Butylthiophene)									
1	-5.604	-0.204	5.400	-11.508	-5.865	5.643	-11.537	-9.246	2.291
2	-5.099	-1.034	4.066	-9.674	-5.394	4.281	-10.340	-8.003	2.337
3	-4.899	-1.420	3.479	-8.703	-5.086	3.617	-9.218	-7.363	1.855
4	-4.795	-1.637	3.158	-8.096	-4.847	3.249	-8.365	-6.964	1.402
5	-4.733	-1.756	2.977	-7.676	-4.633	3.043	-7.780	-6.691	1.089
Poly(3-Hexylthiophene)									
1	-5.595	-0.196	5.399	-10.914	-5.796	5.118	-10.918	-9.188	1.730
2	-5.088	-1.023	4.065	-9.618	-5.347	4.271	-10.173	-7.956	2.217
3	-4.886	-1.408	3.478	-8.654	-5.041	3.613	-9.163	-7.316	1.847
4	-4.785	-1.627	3.158	-8.049	-4.803	3.246	-8.319	-6.917	1.402
Poly(3-Octylthiophene)									
1	-5.590	-0.191	5.399	-10.256	-5.721	4.536	-10.229	-9.136	1.094
2	-5.063	-0.999	4.064	-9.566	-5.309	4.257	-9.765	-7.917	1.848
3	-4.868	-1.389	3.479	-8.635	-5.001	3.634	-9.151	-7.291	1.860
4	-4.764	-1.613	3.151	-8.030	-4.770	3.260	-8.312	-6.892	1.420
Poly(3-Decylthiophene)									
1	-5.588	-0.189	5.399	-10.009	-5.665	4.344	-9.965	-9.102	0.864
2	-5.081	-0.985	4.096	-9.502	-5.302	4.200	-9.545	-7.910	1.635
3	-4.872	-1.371	3.500	-8.625	-4.996	3.629	-9.132	-7.282	1.851
Poly(3-Dodecylthiophene)									
1	-5.599	-0.026	5.573	-9.734	-5.066	4.668	-9.555	-9.049	0.506
2	-5.079	-0.983	4.096	-9.032	-5.283	3.748	-9.031	-7.919	1.112
3	-4.872	-1.395	3.478	-8.610	-4.610	3.633	-8.937	-7.276	1.661

Notes:

<sup>a</sup> neutral sample,<sup>b</sup> with a charge +1 and up-oriented spin,  $S=1/2$ ,<sup>c</sup> with a charge + $e$  and down-oriented spin,  $S= -1/2$ .

## 2.2. DFT structural and band calculations of poly(3-alkylthiophene) oligomers and their composites

Band energy parameters HOMO, LUMO, and  $E_g$ , of P3AT oligomers with different numbers of monomers  $n$ , aromatic and quinoid conformation, in the absence and presence of polarons with spin  $S=1/2$  and positive elementary charge + $e$ , respectively, as well as their composites were numerically calculated in the DFT framework using the Orca v5.0.4 software package [32] with the functional B3LYP [36,37]. This were carried out after preliminary geometry optimization of these systems using the parallel thread data transfer interface (MPI) of a multi-core processor. The population of electron spins and charge density in the

compounds under study were calculated at several geometries using various basis sets and definitions based on the analysis of Mulliken [38] and alternative Löwdin [39] self-consistent field density matrices. These parameters should depend strongly upon basis sets, however, the Mulliken scheme based on an approach of molecular orbitals as linear combination of atomic orbitals performs more satisfactorily than the Löwdin scheme in the case of predominantly ionic molecules [40]. Indeed, the performance of the two schemes becomes comparable for estimation of spin population, whereas the atomic charges calculated within the Löwdin formalism were appeared to be higher considerably than those analyzed within the Mulliken one. Therefore, below are presented the results obtained using the Mulliken approach. Anisotropic

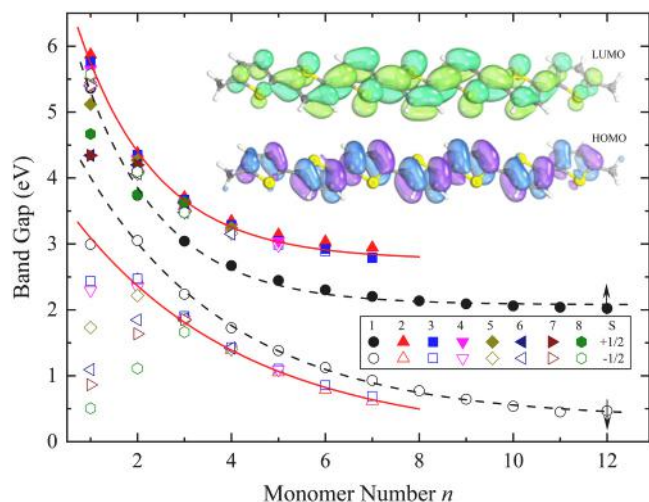


**Fig. 6.** Band gap energy  $E_g = E_{\text{HOMO}} - E_{\text{LUMO}}$  of P3HyT (1), P3MeT (2), P3EtT (3), P3BuT (4), P3HxT (5), P3OcT (6), P3DeT (7), and P3DoT (8) oligomers with both spin  $S = \pm 1/2$  orientation in an external magnetic field and elemental positive charge  $+e$  DFT-calculated according the Mulliken formalism using the Orca software package and procedure described in the Methodical section. In the top are presented the HOMO and LUMO isosurface plots of an exemplary P3HyT oligo7mer. The lines shown from top to bottom were calculated from Eq. (1) with  $a_0 = 2.761$  eV,  $b = 5.447$  eV,  $c = 1.669$ ,  $a_0 = 2.078$  eV,  $b = 5.886$  eV,  $c = 1.671$ ,  $a_0 = 0.347$  eV,  $b = 5.029$  eV,  $c = 3.153$ , and  $a_0 = 0.050$  eV,  $b = 4.003$  eV,  $c = 3.650$ , respectively.

spin-spin hyperfine coupling (HFC) constants  $A$  and Landé  $g$ -factor were determined using the EPRNMR module with the EPRII basis set [41] for nuclei from  $^1\text{H}$  to  $^{12}\text{C}$ . To take into account polaron HFC also with the  $^{32}\text{S}$  nuclei, the additional basis set TZVPP [42] was used as well. To test the effect of the basis set on the calculated EPR parameters, additional single-point calculations were performed using the def2-TZVPP basis set [43] for all atoms, which showed minor differences in the data calculated for the polymer systems under study. Therefore, all parameters presented here were calculated with the EPRII and TZVPP basis sets for both conformers with appropriate spin states and all side substituent atoms. Since no significant effect on the optimized geometry and magnetic resonance parameters was found (as in [24]), all further calculations were assumed to be carried out under vacuum. When calculating the relative changes in main parameters of oligomers, the minimum number  $n$  of their units was chosen equal to seven. Such length of oligomer chain was set to be optimal for obtaining accurate results at optimal computational cost. Visualization of band structures and orbital configurations was performed using the Avogadro v.1.2.0 [44] and MultiWFN v.3.8 [45] programs.

### 2.3. DFT calculation of EPR spectra of poly(3-alkylthiophene) oligomers and their composites

The principal values of the  $\mathbf{A}$ - and  $\mathbf{g}$ -tensors, obtained for oligomers and their composites in the Orca software package, were used for numerical calculation and visualization of respective high-resolution D-band (with  $\nu_e = \omega_e/2\pi = 140$  GHz and  $B_0 = 49960$  G) EPR spectra with using EasySpin v.5.2 software [46]. When modeling the spectra, we took into account an additional anisotropic broadening due to unresolved hyperfine splitting ( $B$ -strain) and also field-dependent  $g$ -strain arising due to distribution of spin Hamiltonian parameters. The calculated EPR spectra were compared with those previously obtained experimentally in our and other labs at millimeter wavebands EPR.

## 3. Results and discussions

### 3.1. Molecular and band structure of poly(3-alkylthiophenes) oligomers

Fig. 2a shows the band diagram of neutral P3AT with the energies of the HOMO and LUMO molecular orbitals separated by a band gap of width  $E_g^0$ . As in the case with the nitrogen atoms of polypyrrole, the  $\pi$ -atomic orbitals of sulfur do not make a corresponding contribution to the HOMO energy level P3HyT [30]. Exposure of a polymer donor-acceptor system, e.g., to photons of visible light initiates intermolecular electron transfer between the HOMO and LUMO energy levels and the formation on the polymer chain of a polaron with a spin and elementary charge  $e$ . This is accompanied by formation in the band gap of the polymer matrix of additional energy sublevels  $E_1$  below the LUMO level and  $E_2$  above the HOMO one (Fig. 2b). The parameters  $E_g^0$ ,  $E_1$ , and  $E_2$  were calculated, e.g., for P3HyT within the Hartree-Fock approximation to be 2.20, 0.71, and 0.61 eV, respectively [30]. If an additional charge leaves the polymer chain, a second similarly charged polaron appears on it, however, with a spin oppositely oriented relative to the external magnetic field (Fig. 2c). This somewhat shifts the position of both sublevels of this double charged carrier. The distance between the indicated sublevels depends on the strength of an external magnetic field  $B_0$ ,  $\Delta E_{12} = E_g^0 - E_1 - E_2 = 2\mu_B B_0 = \gamma_e \hbar B_0$ , where  $\mu_B$  is the Bohr magneton,  $\gamma_e$  is gyromagnetic ratio for an electron, and  $\hbar = h/2\pi$  is the Plank constant. This value calculated for the X- and D-wavebands EPR operating at  $B_0 = 3350$  and 48870 G is 0.039 and 0.574 meV, respectively.

### 3.2. Atomic distribution of spin population and charge density in poly(3-Alkylthiophene) oligomers

Fig. 3 shows the DFT-optimized P3HyT and P3MeT oligo12mers with aromatic and quinoid conformations. The relative values of the positive charge density, as well as the electron spin population, calculated for these compounds in the Mulliken approximation [38], are given for the corresponding  $^1\text{H}$  and  $^{32}\text{S}$  atoms constituting these compounds in a,c and b,d, respectively. From the data shown in Fig. 3a, it is clear that the charge is distributed evenly on the protons of the neutral P3HyT oligomer except for those finalized monomers. A similar case is observed when the third-position hydrogen atoms in the monomers are replaced by methyl groups. This changes significantly when an elemental charge leaves the polymer backbone due to some physical effect. It decreases the dihedral/torsion angle  $\text{S-C}=\text{C-S}$  of neutral P3HyT, the angle of its middle monomer from  $93.86^\circ$  in  $-\text{C-S-C}-$  to  $93.76^\circ$  in  $=\text{C-S-C}=\text{}$ , which is accompanied by stabilization on its chain of a mobile polaron with a quinoid conformation, carrying a charge  $+e$  and spin  $S=1/2$  (Fig. 3b,d). Spin cloud of an unpaired electron is distributed accordingly on all its constituent atoms, however, with the higher density on the terminal hydrogen nuclei. It is important to note that when replacing hydrogen atoms by methyl groups, the spin density on the polaron sulfur atoms,  $\rho(^{32}\text{S})$ , increases by ca. 1.5 times (Fig. 3d).

A clearer change in the electron and spin populations on each atom of the confor12mers P3HyT and P3MeT is demonstrated in Fig. 4, in which each symbol refers to their corresponding hydrogen  $^1\text{H}$ , sulfur  $^{32}\text{S}$  and carbon  $^{12}\text{C}$  atoms. The presented data evidences a uniform charge distribution on most P3HyT atoms. The character of the spin density distribution clearly indicates the presence in the middle of the polymer chain of a polaron with a characteristic length of about seven monomers (Fig. 4b,f,j). This parameter is close to that experimentally obtained under study of this polymer by EPR [9] and Electron Nuclear Double Resonance (ENDOR) [19] methods. As the Figure shows, the uniform distribution of spin density on sulfur atoms  $\rho(^{32}\text{S})$  along the polaron in the P3HyT conformer becomes inhomogeneous as hydrogen atoms are replaced by methyl groups. In this case such parameter changes approximately by one and a half times within the polaron extent. This is accompanied by the appearance of a specific asymmetry in the spin

Table 2

The main and averaged values of spin-spin hyperfine coupling constants  $A_i$  (all in MHz) and  $g$ -tensors calculated for oxidized poly(3-alkylthiophene) oligomers with different both the monomer number  $n$  and side alkyl substituents using the Orca software package according to the procedure described in the Methodical section.

$n$	$A_x$	$A_y$	$A_z$	$A_{iso}$	$g_{xx}$	$g_{yy}$	$g_{zz}$	$g_{iso}$
Poly(3-Hydrothiophene)								
1	34.826	32.965	37.999	35.263	2.001279	2.002066	2.002730	2.002025
2	14.877	12.252	14.206	13.778	2.003815	2.002006	2.000769	2.002197
3	7.172	5.460	6.109	6.247	2.002979	2.002012	2.001398	2.002130
4	4.219	2.028	2.521	2.923	2.003111	2.002021	2.001000	2.002044
5	2.632	0.491	0.562	1.228	2.002906	2.002014	2.000970	2.001963
6	1.704	-0.328	-0.478	0.299	2.002944	2.002007	2.000741	2.001898
7	1.168	-0.743	-1.021	-0.199	2.002857	2.001999	2.000651	2.001836
8	0.819	-0.968	-1.313	-0.487	2.002867	2.001993	2.000528	2.001796
9	0.590	-1.081	-1.451	-0.647	2.002835	2.001975	2.000488	2.001766
10	0.431	-1.133	-1.505	-0.736	2.002854	2.001930	2.000443	2.001742
11	0.332	-1.134	-1.502	-0.768	2.002835	2.001933	2.000443	2.001736
12	0.270	-1.178	-1.524	-0.811	2.00283	2.00191	2.00043	2.001723
Poly(3-Methylthiophene)								
1	30.508	31.452	38.383	33.448	2.003308	2.002041	2.001236	2.002195
2	12.618	12.401	15.871	13.630	2.003305	2.002002	2.001172	2.002160
3	6.861	6.405	8.530	7.265	2.002972	2.002004	2.001382	2.002119
4	4.355	3.866	5.339	4.520	2.003060	2.001993	2.001157	2.002070
5	3.083	2.620	3.736	3.146	2.002985	2.001961	2.001115	2.002020
6	2.417	1.992	2.894	2.434	2.002977	2.001916	2.000967	2.001953
7	1.953	1.566	2.320	1.946	2.002946	2.001946	2.000947	2.001946
Poly(3-Ethylthiophene)								
1	27.088	27.304	32.247	28.880	2.002888	2.002034	2.001358	2.002093
2	9.541	9.548	11.644	10.245	2.003282	2.002016	2.001110	2.002136
3	4.643	4.400	5.742	4.928	2.002964	2.002088	2.001295	2.002116
4	2.660	2.449	3.194	2.768	2.003035	2.002026	2.001113	2.002058
5	1.683	1.545	1.914	1.714	2.002966	2.001949	2.001038	2.001984
6	1.179	0.934	1.315	1.143	2.002980	2.001946	2.000991	2.001972
7	1.331	1.105	1.479	1.306	2.002953	2.001944	2.001006	2.001968
Poly(3-Butylthiophene)								
1	17.260	17.312	20.399	18.324	2.003063	2.001961	2.001322	2.002115
2	5.769	5.511	7.394	6.225	2.003443	2.002091	2.001130	2.002221
3	2.700	2.609	3.539	2.949	2.003445	2.002065	2.000959	2.002156
4	1.527	1.477	1.968	1.657	2.003221	2.002016	2.000959	2.002065
Poly(3-Hexylthiophene)								
1	13.143	14.242	15.419	14.268	2.003134	2.001991	2.001333	2.002153
2	4.331	4.114	5.632	4.692	2.003448	2.002072	2.001140	2.002220
3	2.017	1.861	2.716	2.180	2.003450	2.002063	2.000966	2.002160
Poly(3-Octylthiophene)								
1	9.909	10.424	11.088	10.474	2.003195	2.002008	2.001339	2.002181
2	3.172	3.027	4.079	3.426	2.003324	2.002109	2.001069	2.002167
3	1.598	1.469	2.057	1.708	2.002896	2.002107	2.001296	2.002099
Poly(3-Decylthiophene)								
1	9.068	9.454	9.966	9.496	2.003258	2.002058	2.001358	2.002225
2	2.875	2.735	3.785	3.131	2.003325	2.002110	2.001071	2.002169
Poly(3-Dodecylthiophene)								
1	5.889	5.609	5.810	5.770	2.003601	2.002330	2.001646	2.002526
2	2.474	2.349	3.263	2.695	2.003500	2.002050	2.001186	2.002245

Note: The principal values of  $A$ - and  $g$ -tensors may not coincide.

density distribution cross all oligomer atoms (Fig. 4c,g,k). To explain this effect, the structural and composition impact of the side substituents in polythiophene derivatives on the change in the configuration of the spin cloud should be analyzed. It is known that spin distribution strongly depends on atom interaction with own microenvironment. As it is seen from Fig. 5a, such interaction of the H and C atoms is more heterogeneous in P3AT, therefore they are characterized by saw-shape distribution of spin density. On the other hand, spin cloud on sulfur atoms is more homogeneous, which allows to simplify subsequent analysis. Fig. 5a shows dependences of the spin density distribution on these nuclei in both aromatic and quinoidal P3HyT conformers, and quinoid conformers of some other polythiophene derivatives with various combinations of side substituents, including P3MeT. From the data presented, we can conclude that the asymmetry of the spatial distribution of spin density increases in the 2→1→5→3→4 conformer series. This parameter is also governed by the length of the alkyl substituent  $R$ . Fig. 5b shows the dependences of the spatial distribution of the spin density of polarons initiated in P3AT with  $R = H, CH_3, C_2H_5,$  and  $C_3H_7$ . Analyzing the data obtained, we can conclude that the spin density on

sulfur nuclei monotonically decreases in the  $CH_3 \rightarrow C_2H_5 \rightarrow C_3H_7$  series at unchangeable shape of its spatial distribution along the main oligomer  $x$ -axis. We can also to assume the coexistence in them of the region with faster and slower spin delocalization characterized by broad and narrow contributions, respectively. Fig. 5b demonstrates such contributions and their sum calculated for exemplary P3HyT system. The existence of the second term can be explained, for example, by local pinning of part of topological distortions due to the peculiarities of their formation, relaxation and coupling with own microenvironment, as it is realized in some other conjugated low-dimensional compounds [12,47]. Analyzing the data obtained, it is clear that the largest contribution of more faster spin delocalization is recorded in P3AT conformers with extended alkyl substituents. Integrating both corresponding terms allows one to determine the population ratio of so excited spins, e.g., in the P3MeT to be near 11.2:1.0.

Thus, the proposed procedure makes it possible to precisely handling at the atomic level the structural, conformational, electronic and spin parameters of the polymer compounds under study, as well as other systems based on organic conjugated polymers.

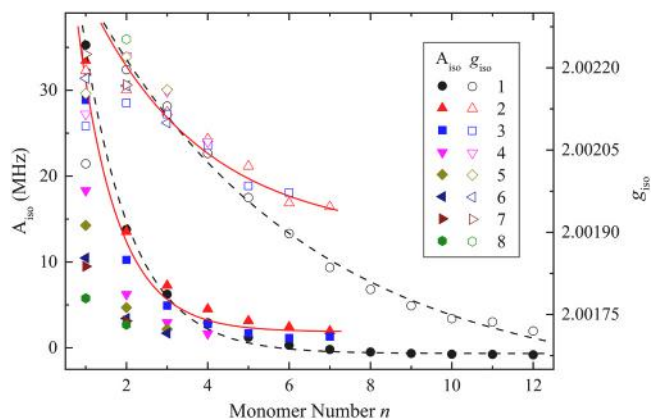


**Fig. 7.** Isotropic constants of spin-spin superfine coupling,  $A_{\text{iso}}$ , and  $g$ -factor,  $g_{\text{iso}}$ , of polaronic charge carriers initiated in the P3HyT (1), P3MeT (2), P3EtT (3), P3BuT (4), P3HxT (5), P3OcT (6), P3DeT (7), P3DoT (8) oligomer chains as functions of their both the unit number  $n$  and alkyl substitute spread. Up-to-down solid lines show dependences calculated from Eq. (1) with  $a_0 = 2.00162$ ,  $b = 8.71 \times 10^{-4}$ ,  $c = 5.31$  and  $a_0 = 0.471$  MHz,  $b = 83.62$  MHz,  $c = 1.17$ , respectively, whereas the similarly ordered dashed lines show curves calculated from the same relation with  $a_0 = 2.00189$ ,  $b = 6.41 \times 10^{-4}$ ,  $c = 2.79$  and  $a_0 = 1.873$  MHz,  $b = 81.31$  MHz,  $c = 0.976$ , respectively.

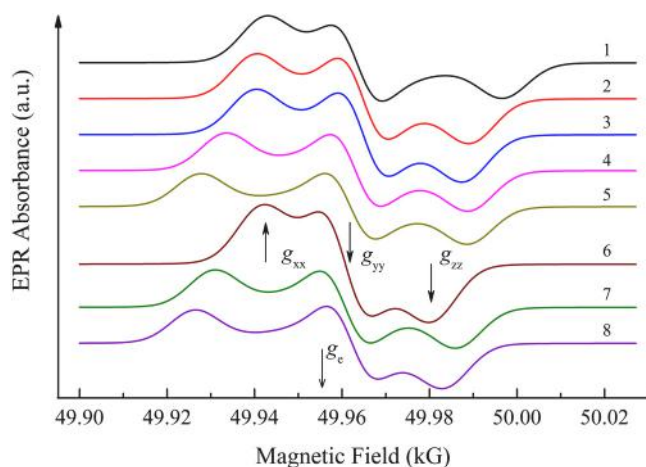


**Fig. 8.** D-Band EPR spectra calculated by the EasySpin program packet for polarons excited in the P3HyT (1), P3MeT (2), P3EtT (3), P3BuT (4), P3HxT (5), P3OcT (6), P3DeT (7), P3DoT (8) oligomer backbones by using their resonant parameters summarized in Table 2 according to the procedure described in the Methodical section. The main values  $g_{ii}$  of their  $g$ -tensor, as well as the  $g$ -factor of free electron  $g_e$ , are shown.

### 3.3. DFT calculation of band structure of P3AT oligomers

The band parameters HOMO, LUMO, and band gap,  $E_g$ , calculated for neutral and oxidized P3AT oligomers under study with different numbers of monomers  $n$  at both polaron spin orientations in an external magnetic field, are summarized in Table 1. The  $E_g$  values determined for these compounds are shown in Fig. 6 as a function of their monomer number  $n$ . One can find out from the data presented a rather expected conclusion about sufficient dependency of the band gap on the number  $n$  of these compounds and also on the state of their polaron spins. These dependencies can be approximated by a simple exponential decay law,

$$a = a_0 + b \cdot \exp(-n/c) \quad (1)$$

where  $a_0$  is the value of the desired parameter for an infinite length of the polymer, i.e. in the  $n \rightarrow \infty$  limit,  $b$  and  $c$  are coefficients. Indeed, the  $E_g(n)$  obtained for the P3HyT oligomer can be approximated by the

dashed upper and lower dependences calculated from law (1) with  $a_0 = 2.078$  eV,  $b = 5.886$  eV,  $c = 1.671$  and  $a_0 = 0.347$  eV,  $b = 5.029$  eV,  $c = 3.153$ , respectively. The upper and lower dependences shown by solid lines, calculated from this Equation with  $a_0 = 2.761$  eV,  $b = 5.447$  eV,  $c = 1.669$  and  $a_0 = 0.050$  eV,  $b = 4.003$  eV,  $c = 3.650$ , also describe quite well the averaged data, obtained for both spin orientations in other P3AT. The  $a_0$  values obtained for P3AT studied are appeared to be quite close to those calculated for P3HyT (2.20 eV) [30] and obtained experimentally for regioregular P3HxT (1.90–2.07 eV) [48–50], P3OcT (1.92 eV), and P3DeT (1.93 eV) [49].

Thus, analysis of the data obtained shows that an increase of polymerization degree squeezes exponentially the band gap of conjugated polymers and their composites. However, replacing hydrogen atoms in the third position with alkyl chains leads to the opposite effect. This may provide an additional opportunity to realize handling of charge transfer processes in respective polymer molecular devices.

### 3.4. DFT calculation of parameters of spin Hamiltonian of P3AT oligomers

The analytical software used in the work made it possible to calculate the main parameters of the spin Hamiltonian, the HFC constant, as well as the Landé  $g$ -factor, which characterize polaron spin state and interaction in the studied P3AT radical cations. These parameters calculated for various P3AT oligomers with different alkyl substituents  $R$  and the number of monomers  $n$  are summarized in Table 2. Fig. 7 shows the dependences of the average/isotropic parameters  $A_{\text{iso}}$  and  $g_{\text{iso}}$  of these systems on the polymerization coefficient  $n$ . The data presented indicate the dependence of the spin Hamiltonian on both these parameters. They can also be approximated by Eq. (1). Indeed, Fig. 7 indicates an exponential dependence of the functions  $g_{\text{iso}}(n)$  and  $A_{\text{iso}}(n)$  with  $a_0 = 2.00162$ ,  $b = 8.71 \times 10^{-4}$ ,  $c = 5.31$  and  $a_0 = 0.471$  MHz,  $b = 83.62$  MHz,  $c = 1.17$ , respectively. Once hydrogen atoms are replaced by alkyl groups, the averaged dependences of the corresponding compounds are also approximated by Eq. (1) with  $a_0 = 2.00189$ ,  $b = 6.41 \times 10^{-4}$ ,  $c = 2.79$  and  $a_0 = 1.873$  MHz,  $b = 81.31$  MHz,  $c = 0.976$ , respectively.

The anisotropic HFC constants and  $g$ -factors obtained for the studied P3AT oligomers in the  $n \rightarrow \infty$  limit were then used to calculate respective high-resolution D-band EPR spectra of these compounds using the EasySpin software package. It would be noted that EPR spectra can be broadened by dynamic effects (relaxation, tumbling, chemical exchange) or static effects (orientational disorder and unresolved hyperfine coupling characterized by  $g$ - and  $A$ -tensors, respectively). Such effects are initiated by small structural variations among the polarons excited in a disordered system and, therefore, they depend on the orientation of a polaron spin in the external magnetic field and should be considered during the simulation of respective EPR spectra. Physical origins for anisotropic field-dependent broadening of EPR spectra of organic polymers are an unresolved hyperfine splitting and a distribution of  $g$  principal values characterized by so-called  $B$ - and  $g$ -strains. The different nature of the spectra broadening was taken into account in the calculations. So then, these strains used for calculation, e.g., of the initial P3HyT oligo12mer were [0.39 1.50 2.63] G and [0.0005 0.0004 0.0005], respectively. EPR spectra calculated for some P3AT oligomers using the data summarized in Table 2 are presented in Fig. 8. It is seen from the Fig. 7a trend for monotonic decrease in both  $A_{\text{iso}}$  and  $g_{\text{iso}}$  parameters of the studied oligomers with an increase in their alkyl substituents length  $R$  and the number of monomers  $n$ . However, such monotonicity is not evident in the shape of the spectra of these compounds. This discrepancy may be due to different conformations of their monomers and, thus, different configurations of the spin cloud in their charge carriers. It is seen from the Fig. 8 that the P3OcT oligomer demonstrate minimal distance between its spectral components with  $g_{xx}$  and  $g_{zz}$ . This indicates less anisotropy of its magnetic resonance parameters due to its better ordering. It may become more pronounced upon possible acceleration of intermolecular coupling in real polymers

**Table 3**

Band parameters HOMO, LUMO, and  $E_g$  (all in eV) calculated for the initial and oxidized poly(3-hydrothiophene) and poly(3-methylthiophene) oligo7mers modified with different polyacenes (PA), triphenyls (TP), and polycyclic aromatic hydrocarbons (PH) additives with extended  $\pi$ -conjugated systems calculated using Orca software package as it is described in the Methodical section.

Additive	HOMOA	LUMOA	$E_g^a$	HOMOB	LUMOB	$E_g^b$	HOMOA	LUMOA	$E_g^a$	HOMOB	LUMOB	$E_g^b$
	Poly(3-Hydrothiophene)						Poly(3-Methylthiophene)					
–	-6.961	-5.132	1.829	-7.194	-6.075	1.118	-6.672	-4.810	1.862	-6.900	-5.772	1.128
PA1	-6.918	-5.095	1.823	-7.163	-6.025	1.137	-6.637	-4.779	1.858	-6.876	-5.732	1.144
PA2	-6.875	-5.064	1.812	-7.131	-5.986	1.145	-6.609	-4.760	1.850	-6.860	-5.703	1.157
PA3	-6.867	-5.053	1.818	-7.012	-5.971	1.041	-6.593	-4.749	1.844	-6.841	-5.688	1.153
PA4	-6.712	-4.992	1.720	-6.792	-5.899	0.893	-6.530	-4.724	1.806	-6.665	-5.657	1.008
PA5	-6.409	-5.008	1.401	-6.400	-5.894	0.506	-6.346	-4.753	1.594	-6.342	-5.656	0.686
PA6	-6.562	-4.890	1.672	-6.472	-5.809	0.663	-6.398	-4.652	1.747	-6.366	-5.587	0.779
PA7	-6.383	-4.912	1.470	-6.387	-5.823	0.564	-6.338	-4.638	1.699	-6.262	-5.574	0.688
PA8	-6.375	-4.881	1.494	-6.332	-5.785	0.547	-6.285	-4.617	1.669	-6.271	-5.550	0.720
PA9	-6.329	-4.870	1.459	-6.258	-5.763	0.495	-6.256	-4.597	1.659	-6.257	-5.539	0.718
PA10	-6.286	-4.860	1.426	-6.257	-5.759	0.498	-6.017	-5.467	0.550	-6.250	-4.976	1.274
TP4	-6.834	-5.010	1.824	-7.096	-5.941	1.155	-6.564	-4.700	1.865	-6.798	-5.661	1.136
TP7	-6.778	-4.973	1.805	-7.050	-5.878	1.172	-6.519	-4.661	1.858	-6.757	-5.617	1.140
TP10	-6.536	-4.890	1.646	-6.536	-5.819	0.717	-6.447	-4.612	1.834	-6.470	-5.570	0.899
TP13	-6.253	-4.720	1.533	-6.245	-5.671	0.574	–	–	–	–	–	–
PH5	-6.810	-4.998	1.813	-6.798	-5.921	0.877	-6.602	-4.700	1.902	-6.758	-5.713	1.044
PH6	-6.737	-4.987	1.750	-6.728	-5.934	0.793	-6.542	-4.700	1.842	-6.690	-5.638	1.052
PH7	-6.811	-4.988	1.822	-7.059	-5.913	1.146	-6.559	-4.693	1.865	-6.786	-5.649	1.137
PH8	-6.514	-5.085	1.429	-6.405	-5.788	0.617	-6.369	-4.700	1.669	-6.357	-5.637	0.719
PH9	-6.564	-4.958	1.606	-6.547	-5.882	0.665	-6.459	-4.667	1.792	-6.454	-5.623	0.831
PH10	-6.774	-4.987	1.787	-6.780	-5.883	0.897	-6.540	-4.670	1.870	-6.718	-5.631	1.087
PH11	-6.497	-4.884	1.613	-6.462	-5.828	0.634	-6.488	-4.633	1.855	-6.638	-5.591	1.047
PH12	-6.464	-4.972	1.492	-6.380	-5.774	0.607	-6.204	-4.750	1.454	-6.190	-5.581	0.609
PH13	-6.497	-4.884	1.613	-6.462	-5.827	0.635	-6.352	-4.638	1.714	-6.352	-5.592	0.760
PH14	-6.583	-4.920	1.663	-6.584	-5.843	0.740	-6.508	-4.641	1.867	-6.551	-5.590	0.961
PH15	-6.349	-4.877	1.472	-6.323	-5.755	0.568	–	–	–	–	–	–
PH16	-6.323	-4.843	1.480	-6.311	-5.790	0.521	–	–	–	–	–	–
PH17	-6.542	-4.944	1.598	-6.534	-5.840	0.694	–	–	–	–	–	–
PH18	-6.620	-4.939	1.681	-6.614	-5.836	0.778	–	–	–	–	–	–
PH19	-6.657	-4.902	1.755	-6.695	-5.823	0.872	–	–	–	–	–	–
PH20	-6.291	-4.814	1.477	-6.313	-5.747	0.566	–	–	–	–	–	–

Note: The index of samples means a number of phenyl circles.

and their composites. The calculated magnetic resonance parameters lie nearby to those determined experimentally for some neutral and modified P3AT [20,21,24,49,51,52].

### 3.5. Structure improving of composites stipulated by polycyclic aromatic hydrocarbons

Previously [34,35], it was found that the electronic and spin properties of P3DoT donor-acceptor composites depend on the band gap of aromatic polycyclic Q1D-hydrocarbon additives embedded into polymer matrix. A few molecules embedded into organic compounds was appeared to play a role of centers forming crystallization phase of their active matrix. It improves the morphology of the composite and, thereby, increases its functionality. Below are analyzed the influence of the structure, composition and dimensionality of different Q1D polyacenes, triphenylenes, and Q2D polyaromatic graphene-like hydrocarbons shown in Fig. 1 on the electronic parameters and spin state of polarons excited in exemplary P3HyT and P3MeT oligomers.

Table 3 presents the main band parameters, HOMO, LUMO, and  $E_g$ , calculated for P3HyT and P3MeT oligo7mers modified with different neutral additives at parallel and opposite spin orientation relative to the external magnetic field. The same parameters, calculated for optimized polycyclic aromatic additives PA, TP, and PH with different numbers of benzene rings  $n$  are summarized in Table S-1 of the Supplementary material. Fig. 9a shows how changes the spin density on sulfur atoms,  $\rho(^{32}S_c) - \rho(^{32}S_0)$ , of the exemplary P3HyT composite when varying the conjugated ring number  $n$  of embedded polycyclic aromatic additives PA, TP, and PH. The choice of this parameter for such an analysis seems to be due to the greater simplicity in the further interpretation due to the lower interaction of these nuclei with own microenvironment. Indeed, if the polaron spin might interact with the sulfur nuclei, similar to that as it

is realized, for example, in benzo-1,2,3-trithiol radical cations, then an effective  $g$ -factor of the corresponding compound would be over 2.014 [53], which is significantly higher than the similar parameter of the spin charge carriers in the oligomers under study. An analysis of the change in spin density on the  $^{32}S$  atoms of the composite reveals its nontrivial dependence on the size of nanoadditives used. It is seen that the composite demonstrates approximately equidistant “extrema” of the function  $\rho(^{32}S_c)$  on the  $n$  value with a distance  $\Delta n \approx 4$  between them. Fig. 9b shows the change in the band gap of this complex depending on the type and size of the polycyclic additives used. It is clear seen from the data presented that the  $E_g$  value of the oligomer, as expected, decreases monotonically in the case of its PA complex with a small (2–3) number of its conjugated rings. Previously, a similar effect was experimentally registered in the study of photovoltaic complexes based on P3DoT [34, 35] and other conjugated polymers [54]. Therefore, it would be quite logical to expect a further monotonic decrease in the energy  $E_g$  in the limit  $n \rightarrow \infty$ . However, it was not to be the case. It was found that instead of this the  $E_g$  value of both oligomer composites and both spin orientation containing PA and PH additives with  $n > 3$  changes in a variable manner. It should be noted that this effect is more pronounced when using P3HyT as a composite matrix and PH as a Q2D-additive. It seems rather ambiguously in the case of both polymer complexes modified with triphenyls, possibly due to the triple discreteness of changes in the number of their rings  $n$ . However, the “extrema” of this dependence do not coincide with those of the above mention function  $\rho(^{32}S_c)$  on the  $n$  value. Analyzing the data presented in Fig. 9b, one can also notice the appearance of a specific periodicity in the change of the function  $E_g(n)$  with a specific step  $\Delta n$ , close to forth phenyl circles. This peculiarity is somewhat reduced with complexes with the P3MeT oligomer as a matrix because, possible, covalent s-bonds in P3HyT are replaced by  $sp^3$ -ones in P3AT with alkyl group that inhibits intermolecular spin-spin coupling. A

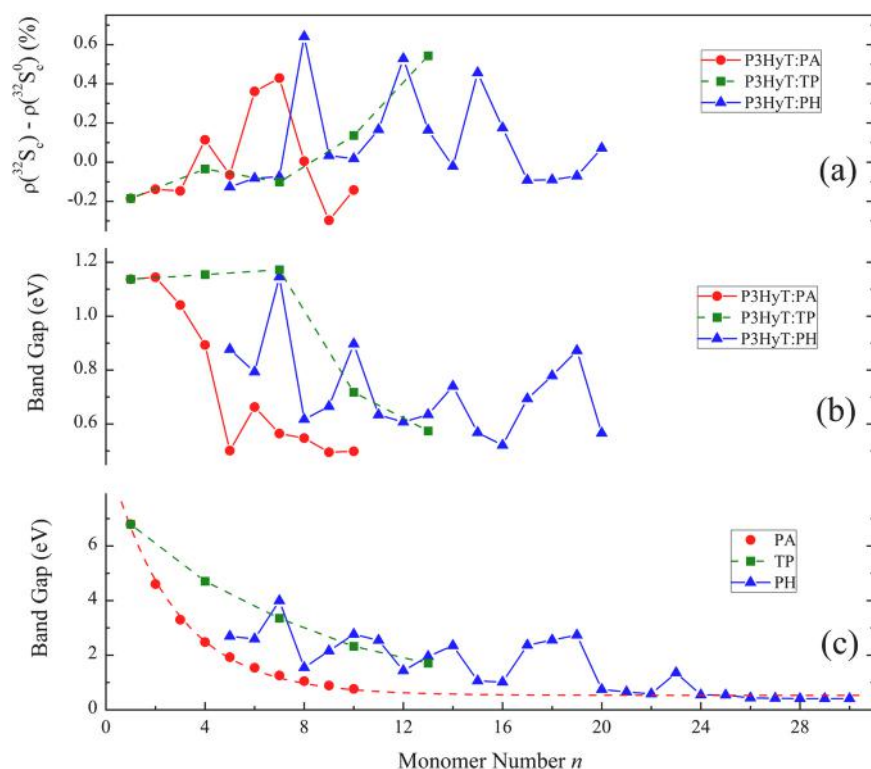


**Fig. 9.** (a) Variation of spin density on  $^{32}\text{S}$  sulfur nuclei in polarons extended along the P3HyT:PA, P3HyT:TP, and P3HyT:PH composites' chains with the parameter  $n$ ; (b) the band gap of the P3HyT:PA, P3HyT:TP, and P3HyT:PH oligo7mer complexes as a function of the number  $n$  of the additives' phenyl rings; (c) band gap of Q1D PA, TP, and Q2D PH aromatic molecules depending on the number of their phenyl rings  $n$ . The dotted line calculated from Eq. (1) with  $a_0 = 0.532$  eV,  $b = 8.968$  eV, and  $c = 2.647$  is shown for the guide of the eye.

slight deviation in functional extrema may be as a result of a scatter in the orientations of molecular planes, as well as the structural molecular asymmetry of PH molecules. Besides, when oligomer and graphene-like molecule form complex, an effective density of states at its Fermi level changes analogously to that how it happens in other interfaces [15, 55, 56]. It initiated slight broadening and shift of respective energetic sub-levels  $E_1$  and  $E_2$  in the matrix band gap. This effect can be attributed, for example, to the splitting of these levels as in the case of half-filled pseudospin-degenerate states at the graphene's Fermi level [57] and also should be taken into account when analyzing the results obtained. One can try to find a possible relationship between the structural, electronic and spin parameters of the complexes under study. Fig. 9c shows how changes the band gaps of neutral PA, TP, and PH nano-additives with variation of their parameter  $n$ . As is known, 2D graphene *a priori* has no band gap, e.g.,  $E_g = 0$  at  $n \rightarrow \infty$ . However, a band gap between the valence and conduction bands of some graphene-like Q2D films of limited size typical for dielectrics and wide-gap semiconductors can in principle be formed. For example, the  $E_g$  value of graphene oxide can vary within 1.7–2.7 eV region depending on its modification level [58]. Besides, this parameter may become non-zero when changing the Q2D film to a chair configuration. It should be taken into account also the presence in the PH additives of side hydrogen atoms. Extrapolation of this parameter PA gives  $E_g = 0.53$  eV at  $n \rightarrow \infty$  (see Fig. 9c), that may mean that the configuration takes an intermediate value. An interesting fact was the change in  $E_g(n)$  of neutral PH molecules with a period of about 4 phenyl rings, possibly due to their Q2D structural degeneracy, which was not manifested in the case of Q1D PA molecules. Note that the described unusual effects were also confirmed by some independent calculations.

From the analysis of the data shown in Fig. 9, a number of important conclusions can be made. First, low-dimensional aromatic additives affect the spin state and interaction of polaron charge carriers with own microenvironment in P3AT-based composites. This effect is explained by

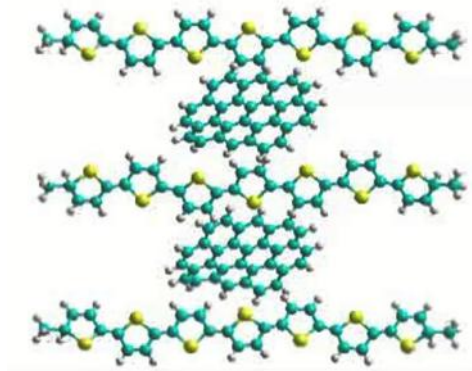
the shielding of the  $\pi$ -interaction of molecular additives with oligomer chains whose alkyl side substituents inhibit intermolecular spin-spin interaction. Secondly, the band gaps and spin population  $\rho(^{32}\text{S}_c)$  of the composites studied vary symbatically and antipatically with the additive polymerization factor  $n$ , respectively. Finally, the data obtained allows us to make the third, main conclusion about possible periodical modulation of the band gap and spin state of the studied composites, varying the dimensionality and polymerizing order of embedded aromatic nanoadditives. This fact should clearly indicate structural and electronic rearrangements initiated in oligomers by such nanoadditives with a periodic molecular  $\pi$ -conjugated structure. This feature can be used, for example, in the development of molecular spintronic sensors and filters with spin-dependent linear (at small values of  $n$ ) and selective (at  $n \geq 4$ ) handling of electronic parameters.

Figure S-1 of the Supplementary material shows exemplary D-band EPR spectra of some P3AT-based composites. They also were calculated in the EasySpin software package using respective eigenvalues of  $\mathbf{A}$ - and  $\mathbf{g}$ -tensors summarized in Table S-2 of the Supplementary material. Analyzing the EPR spectra presented, it can be argued that the introduction of additives into the P3HyT oligomer leads to obvious change in magnetic resonance parameters of polarons initiated in respective complexes, however, the shape of these spectra remains almost unchanged with increasing value  $n$ . On the other hand, the magnetic resonance parameters of polarons in the P3MeT oligomer remain almost unchanged upon embedding of aromatic additive. The spectral extend of these complexes seems to be noticeably less than that of P3AT oligomers with different alkyl substituents (see Fig. 8). The Movie M-1 in Supplementary material demonstrates self-assembly crystallization of an exemplary P3AT matrix due to spin-assisted  $\pi$ - $\pi$ -coupling with aromatic additive.

#### 4. Conclusions

In this paper are reported the data obtained in the DFT and EPR study of electronic and spin parameters of polarons excited in various P3AT oligomers and their complexes with low-dimensional polyaromatic acenes, triphenylenes, and hydrocarbons. The results mainly obtained on exemplary P3HyT and P3MeT oligomers indicate a narrowing of band gap and an increase in planarity as a result of external influence, e. g., illumination. This is accompanied by formation on a chain of a mobile polaron with elemental charge and spin delocalized onto several monomers with quinoidal conformation. Such transition enhances the hyperfine interaction of spin charge carriers with their microenvironment and accelerates spin/charge delocalization along and between Q1D chains of the polymer matrix. It is shown the coexistence in oligomers of conformations with differently delocalized spins whose contributions are determined by the composition and structure of the thiophene side substituents. All spin-assisted processes should to govern the functionality and efficiency of corresponding molecular devices.

The influence of aromatic molecular low-dimensional additives on the electronic and magnetic properties of polarons stabilized on chains of polymer oligomers was analyzed and respective correlations were identified. Hybridization at the interface between different organic systems leads to drastic changes of their structure and magnetic properties stipulated spin polarized states and dramatic effects on spin and charge injection through spinterface. This makes it possible to control its morphology and thereby its electronic and spin parameters. Continuous and specific periodical modulation of these properties by respective aromatic Q1D and Q2D nanoadditives was first registered. This effect opens up new horizons for the development of linear and selective molecular electronic and spintronic devices with spin-dependent parameters. The applicability of the established effects and patterns for other groups of polymer materials was assessed. So, the procedure used



**Video 1.** A video clip is available online. [Supplementary material](https://doi.org/10.1016/j.synthmet.2024.117596) related to this article can be found online at [doi:10.1016/j.synthmet.2024.117596](https://doi.org/10.1016/j.synthmet.2024.117596).

in the work allows precise versatile handle at the atomic level the structural, conformational, electronic and spin parameters of conjugated polymers and their compounds. It needs to be evolved in the further experimental investigation of charge transport cross spinterface of polymer composites under various physical influences.

#### Declaration of Competing Interest

The authors declare that they have no known competing financial interests or personal relationships that could have appeared to influence the work reported in this paper

#### Data availability

No data was used for the research described in the article.

#### Acknowledgments

This work was performed according the State Assignment, No. AAAA-A19-119032690060-9 / FFSG-2024-0010.

#### Supplementary Material

1. Band parameters, HOMO, LUMO, and  $E_g$ , calculated for neutral polyacene (PA), triphenyle (TP), and polycyclic aromatic hydrocarbon (PH) additives.
2. D-Band EPR spectra of polarons initiated in the initial and PA-modified P3HyT and P3MeT oligomers.
3. The main and averaged/isotropic values of spin-spin hyperfine coupling constants  $A_i$  and  $g$ -tensors calculated for the initial and some PA-modified P3HyT and P3MeT oligo7mer complexes.
4. Self-assembly crystallization of the P3HyT:PH10 complex due to spin-assisted intermolecular  $\pi$ - $\pi$ -coupling.

#### Appendix A. Supporting information

Supplementary data associated with this article can be found in the online version at [doi:10.1016/j.synthmet.2024.117596](https://doi.org/10.1016/j.synthmet.2024.117596).

#### References

- [1] W. Hu (Ed.), *Organic Optoelectronics*, Wiley-VCH Verlag Weinheim, 2013.
- [2] M.C. Petty, *Organic and Molecular Electronics: From Principles to Practice*, Wiley-Blackwell, 2018.
- [3] S. Khalifeh, *Polymers in Organic Electronics. Polymer Selection for Electronic, Mechatronic, and Optoelectronic Systems*, ChemTec Publishing, Toronto, 2020.
- [4] S.H. Domingues, R.V. Salvatierra, M.M. Oliveira, A.J.G. Zarbin, Transparent and conductive thin films of graphene/polyaniline nanocomposites prepared through interfacial polymerization, *Chem. Commun.* 47 (2011) 2592–2594, <https://doi.org/10.1039/C0CC04304D>.
- [5] C. Bora, S.K. Dolui, Interfacial synthesis of polypyrrole/graphene composites and investigation of their optical, electrical and electrochemical properties, *Polym. Int.* 63 (2014) 1439–1446, <https://doi.org/10.1002/pi.4635>.
- [6] M.J.T. Raaijmakers, N.E. Benes, Current trends in interfacial polymerization chemistry, *Prog. Polym. Sci.* 63 (2016) 86–142, <https://doi.org/10.1016/j.progpolymsci.2016.06.004>.
- [7] A. Chatterjee, S. Mukhopadhyay (Eds.), *Polarons and Bipolarons: An Introduction*, CRC Press, Boca Raton, 2018.
- [8] R.L. Elsenbaumer, L.W. Shacklette, Phenylene-Based conducting polymers, in: T. E. Scothorn (Ed.), *Handbook of Conducting Polymers*, Marcel Dekker, Inc, New York, 1986, pp. 213–263 (Ch).
- [9] F. Devreux, F. Genoud, M. Nechtschein, B. Villeret, On polaron and bipolaron formation in conducting polymers, in: H. Kuzmany, M. Mehring, S. Roth (Eds.), *Electronic Properties of Conjugated Polymers*, Springer-Verlag, Berlin, 1987, pp. 270–276 (Ch).
- [10] M. Westerling, R. Osterbacka, H. Stubb, Recombination of long-lived photoexcitations in regioregular polyalkylthiophenes, *Phys. Rev. B* 66 (2002) 165220, <https://doi.org/10.1103/PhysRevB.66.165220>.
- [11] S.S. Zade, M. Bendikov, Theoretical Study of Long Oligothiophene Dications: Bipolaron vs Polaron Pair vs Triplet State, *J. Phys. Chem. B* 110 (2006) 15839–15846, <https://doi.org/10.1021/jp062748v>.
- [12] S.A. Brazovskii, S.I. Matveenko, Space-Time Distributions of Solitons and Dislocations in Charge-Density Waves, *J. Exp. Theor. Phys.* 102 (1992) 146–162.
- [13] A.S. Alexandrov (Ed.), *Polarons in Advanced Materials*, Springer, 2007.
- [14] R.I. Eglitis, Ab initio calculations of SrTiO<sub>3</sub>, BaTiO<sub>3</sub>, PbTiO<sub>3</sub>, CaTiO<sub>3</sub>, SrZrO<sub>3</sub>, PbZrO<sub>3</sub> and BaZrO<sub>3</sub> (001), (011) and (111) surfaces as well as F centers, polarons, KTN solid solutions and Nb impurities therein, *Int. J. Mod. Phys. B* 28 (2014) 1430009, <https://doi.org/10.1142/s0217979214300096>.
- [15] Z.V. Vardeny (Ed.), *World Scientific Reference on Spin in Organics. Spin Injection and Transport*, vol. 1, World Scientific Publishing, Singapore, 2018.
- [16] M. Cinchetti, V.A. Dediu, L.E. Hueso, Activating the molecular spinterface, *Nat. Mater.* 16 (2017) 507–515, <https://doi.org/10.1038/nmat4902>.
- [17] C. Boehme (Ed.), *World Scientific Reference on Spin in Organics. Spinterface*, vol. 2, World Scientific Publishing, Singapore, 2018.
- [18] I. Bergenti, V. Dediu, Spinterface: A new platform for spintronics, *Nano Mater. Sci.* 1 (2019) 149–155, <https://doi.org/10.1016/j.nanoms.2019.05.002>.
- [19] S. Kuroda, K. Marumoto, T. Sakanaka, N. Takeuchi, Y. Shimoi, S. Abe, H. Kokubo, T. Yamamoto, Electron-nuclear double-resonance observation of spatial extent of polarons in polythiophene and poly(3-alkylthiophene), *Chem. Phys. Lett.* 435 (2007) 273–277, <https://doi.org/10.1016/j.cplett.2006.12.101>.
- [20] A. Aguirre, P. Gast, S. Orlinski, I. Akimoto, E.J.J. Groenen, H. El Mkami, E. Goovaerts, S. Van Doorslaer, Multifrequency EPR analysis of the positive polaron in I<sub>2</sub>-doped poly(3-hexylthiophene) and in poly[2-methoxy-5-(3,7-

- dimethyloxy)]-1,4-phenylenevinylene, *Phys. Chem. Chem. Phys.* 10 (2008) 7129–7138, <https://doi.org/10.1039/b811419f>.
- [21] A. Konkin, U. Ritter, P. Scharff, H.-K. Roth, A. Aganov, N.S. Sariciftci, D.A.M. Egbe, Photo-induced charge separation process in (PCBM-C<sub>120</sub>O)/(M3EH-PPV) blend solid film studied by means of X- and K-bands ESR at 77 and 120 K, *Synth. Met.* 160 (2010) 485–489, <https://doi.org/10.1016/j.synthmet.2009.11.036>.
- [22] V.I. Krinichnyi, *Multi Frequency EPR Spectroscopy of Conjugated Polymers and Their Nanocomposites*, CRC Press Taylor & Francis Group, Boca Raton, FL, 2016.
- [23] J. Niklas, O.G. Poluektov, Charge transfer processes in OPV materials as revealed by EPR spectroscopy, *Adv. Energy Mater.* 7 (2017) 1602226, <https://doi.org/10.1002/aenm.201602226>.
- [24] M. Van Landeghem, W. Maes, E. Goovaerts, S. Van Doorslaer, Disentangling overlapping high-field EPR spectra of organic radicals: Identification of light-induced polarons in the record fullerene-free solar cell blend PBDB-T:ITIC, *J. Magn. Reson.* 288 (2018) 1–10, <https://doi.org/10.1016/j.jmr.2018.01.007>.
- [25] K.-u.-R. Naveed, L. Wang, H. Yu, R.S. Ullah, M. Haroon, S. Fahad, J. Li, T. Elshaarani, R.U. Khan, A. Nazir, Recent progress in the electron paramagnetic resonance study of polymers, *Pol. Chem.* 9 (2018) 3306–3335, <https://doi.org/10.1039/C8PY00689J>.
- [26] S. Millefiori, A. Alparone, A. Millefiori, Conformational properties of thiophene oligomers, *J. Heterocycl. Chem.* 37 (2000) 847–853, <https://doi.org/10.1002/jhet.5570370429>.
- [27] N.S. Sariciftci, Dynamic orientation of oligothiophenes in nematic liquid crystalline matrices, *Synth. Met.* 80 (1996) 137–141.
- [28] F.J. Heremans, C.G. Yale, D.D. Awschalom, Control of Spin Defects in Wide-Bandgap Semiconductors for Quantum Technologies, *Proc. IEEE* 104 (2016) 2009–2023, <https://doi.org/10.1109/JPROC.2016.2561274>.
- [29] W. Kohn, Nobel Lecture: Electronic structure of matter—wave functions and density functionals, *Rev. Mod. Phys.* 71 (1999) 1253–1266, <https://doi.org/10.1103/RevModPhys.71.1253>.
- [30] J.L. Brédas, B. Themans, J.G. Fripiat, J.M. Andre, R.R. Chance, Highly conducting polyparaphenylene, polypyrrole, and polythiophene chains: An *ab initio* study of the geometry and electronic-structure modifications upon doping, *Phys. Rev. B* 29 (1984) 6761–6773, <https://doi.org/10.1103/PhysRevB.29.6761>.
- [31] M. Springborg, The electronic-properties of polythiophene, *J. Phys.* 4 (1992) 101–120.
- [32] F. Neeze, The ORCA program system, *WIREs Comput. Mol. Sci.* 2 (2012) 73–78, <https://doi.org/10.1002/wcms.81>.
- [33] J. Niklas, K.L. Mardis, B.P. Banks, G.M. Grooms, A. Sperlich, V. Dyakonov, S. Beauprè, M. Leclerc, T. Xu, L. Yue, O.G. Poluektov, Highly-efficient charge separation and polaron delocalization in polymer–fullerene bulk-heterojunctions: a comparative multi-frequency EPR and DFT study, *Phys. Chem. Chem. Phys.* 15 (2013) 9562–9574, <https://doi.org/10.1039/C3CP51477C>.
- [34] V.I. Krinichnyi, E.I. Yudanov, N.N. Denisov, V.R. Bogatyrenko, Effects of small-molecule-doping on spin-assisted processes in P3DDT:PC<sub>61</sub>BM photovoltaics, *Synth. Met.* 267 (2020) 116462, <https://doi.org/10.1016/j.synthmet.2020.116462>.
- [35] V.I. Krinichnyi, E.I. Yudanov, N.N. Denisov, Light-Induced EPR Study of Polymorphic Acene-Stipulated Transition in P3DDT:PC<sub>61</sub>BM Composite, *J. Phys. Chem. C* 126 (2022) 4495–4507, <https://doi.org/10.1021/acs.jpcc.1c10407>.
- [36] A.D. Becke, Density-functional exchange-energy approximation with correct asymptotic behavior, *Phys. Rev. A* 38 (1988) 3098–3100, <https://doi.org/10.1103/PhysRevA.38.3098>.
- [37] C. Lee, W. Yang, R.G. Parr, Development of the Colle-Salvetti correlation-energy formula into a functional of the electron density, *Phys. Rev. B* 37 (1988) 785–789, <https://doi.org/10.1103/PhysRevB.37.785>.
- [38] R.S. Mulliken, Electronic Population Analysis on LCAO-MO Molecular Wave Functions. IV. Bonding and Antibonding in LCAO and Valence-Bond Theories, *J. Chem. Phys.* 23 (2004) 2343–2346, <https://doi.org/10.1063/1.1741877>.
- [39] P.-O. Löwdin, On the Nonorthogonality Problem, in: P.-O. Löwdin (Ed.), *Adv. Quantum Chem.*, Academic Press, 1970, pp. 185–199 (Ch).
- [40] T. Kar, A.B. Sannigrahi, Effect of basis set on Mulliken and Löwdin atomic charges, bond orders and valencies of some polar molecules, *J. Mol. Struct.* 165 (1988) 47–54, [https://doi.org/10.1016/0166-1280\(88\)87005-2](https://doi.org/10.1016/0166-1280(88)87005-2).
- [41] V. Barone, Structure, magnetic properties and reactivities of open-shell species from density functional and self-consistent hybrid methods, in: D.P. Chong (Ed.), *Recent Advances in Density Functional Methods*, World Scientific Publishing, River Edge, London, 1995, pp. 287–334. Ch. 8.
- [42] A. Schäfer, H. Horn, R. Ahlrichs, Fully optimized contracted Gaussian basis sets for atoms Li to Kr, *J. Chem. Phys.* 97 (1992) 2571–2577, <https://doi.org/10.1063/1.463096>.
- [43] J. Zheng, X. Xu, D.G. Truhlar, Minimally augmented Karlsruhe basis sets, *Theor. Chem. Acc.* 128 (2011) 295–305, <https://doi.org/10.1007/s00214-010-0846-z>.
- [44] M.D. Hanwell, D.E. Curtis, D.C. Lonie, T. Vandermeersch, E. Zurek, G.R. Hutchison, Avogadro: an advanced semantic chemical editor, visualization, and analysis platform, *J. Cheminform.* 4 (2012) 17, <https://doi.org/10.1186/1758-2946-4-17>.
- [45] T. Lu, F. Chen, Multiwfn: A multifunctional wavefunction analyzer, *J. Comput. Chem.* 33 (2012) 580–592, <https://doi.org/10.1002/jcc.22885>.
- [46] S. Stoll, A. Schweiger, EasySpin, a comprehensive software package for spectral simulation and analysis in EPR, *J. Magn. Reson.* 178 (2006) 42–55, <https://doi.org/10.1016/j.jmr.2005.08.013>.
- [47] S. Brazovskii, T. Nattermann, Pinning and sliding of driven elastic systems: from domain walls to charge density waves, *Adv. Phys.* 53 (2004) 177–252, <https://doi.org/10.1080/00018730410001684197>.
- [48] D.H. Kim, Y.D. Park, Y.S. Jang, H.C. Yang, Y.H. Kim, J.I. Han, D.G. Moon, S.J. Park, T.Y. Chang, C.W. Chang, M.K. Joo, C.Y. Ryu, K.W. Cho, Enhancement of field-effect mobility due to surface-mediated molecular ordering in regioregular polythiophene thin film transistors, *Adv. Funct. Mater.* 15 (2005) 77–82.
- [49] S. Sensfuss, M. Al-Abraham, Optoelectronic properties of conjugated polymer/fullerene binary pairs with variety of LUMO level differences, in: S.S. Sun, N. S. Sariciftci (Eds.), *Organic Photovoltaics: Mechanisms, Materials, and Devices (Optical Engineering)*, CRC Press, Boca Raton, 2005, pp. 529–557 (Ch).
- [50] C. Enengl, S. Enengl, S. Pluczyk, M. Havlicek, M. Lapkowski, H. Neugebauer, E. Ehrenfreund, Doping-Induced Absorption Bands in P3HT: Polaron and Bipolarons, *ChemPhysChem* 17 (2016) 3836–3844, <https://doi.org/10.1002/cphc.201600961>.
- [51] P. Bernier, The magnetic properties of conjugated polymers: ESR studies of undoped and doped systems, in: T.E. Scotheim (Ed.), *Handbook of Conducting Polymers*, Marcel Dekker, Inc, New York, 1986, pp. 1099–1125 (Ch.).
- [52] V.I. Krinichnyi, EPR spectroscopy of polymer:fullerene nanocomposites, in: S. Thomas, D. Rouxel, M. Ponnanna (Eds.), *Spectroscopy of Polymer Nanocomposites*, 1 ed., Elsevier, Amsterdam, 2016, pp. 202–275. Ch. 9.
- [53] V.I. Krinichnyi, R. Herrmann, E. Fanghänel, W. Mörke, K. Lüders, Spin relaxation and magnetic properties of benzo-1,2,3-trithiolium radical cations, *Appl. Magn. Reson.* 12 (1997) 317–327, <https://doi.org/10.1007/BF03162198>.
- [54] V.I. Krinichnyi, E.I. Yudanov, N.N. Denisov, A.A. Konkin, U. Ritter, V. R. Bogatyrenko, A.L. Konkin, Light-Induced Electron Paramagnetic Resonance study of charge transport in fullerene and nonfullerene PBDB-T-based solar cells, *J. Phys. Chem. C* 125 (2021) 12224–12240, <https://doi.org/10.1021/acs.jpcc.1c03427>.
- [55] S. Sanvito, The rise of spinterface science, *Nat. Phys.* 6 (2010) 562–564, <https://doi.org/10.1038/nphys1714>.
- [56] F. Djeghloul, F. Ibrahim, M. Cantoni, M. Bowen, L. Joly, S. Boukari, P. Ohresser, F. Bertran, P. Le Fèvre, P. Thakur, F. Scheurer, T. Miyamachi, R. Mattana, P. Seneor, A. Jaafar, C. Rinaldi, S. Javaid, J. Arabski, J.P. Kappler, W. Wulfhekel, N.B. Brookes, R. Bertacco, A. Taleb-Ibrahimi, M. Alouani, E. Beaurepaire, W. Weber, Direct observation of a highly spin-polarized organic spinterface at room temperature, *Sci. Rep.* 3 (2013) 1272, <https://doi.org/10.1038/srep01272>.
- [57] A. Zhou, W. Sheng, Abnormal pseudospin-degenerate states in a graphene quantum dot with double vacancy defects, *J. Appl. Phys.* 112 (2012) 014308, <https://doi.org/10.1063/1.4732075>.
- [58] H.K. Jeong, M.H. Jin, K.P. So, S.C. Lim, Y.H. Lee, Tailoring the characteristics of graphite oxides by different oxidation times, *J. Phys. D: Appl. Phys.* 42 (2009) 065418, <https://doi.org/10.1088/0022-3727/42/6/065418>.